Light bending in curved plasma channels

A. J. W. Reitsma and D. A. Jaroszynski
Department of Physics, University of Strathclyde, Glasgow, G4 0NG, UK

Main contact email address **a.reitsma@phys.strath.ac.uk**

Introduction

Plasma channels play an important role in laser-plasma interaction, as they offer a practical solution to the problem of extending the interaction length beyond the limit set by geometric diffraction [1,2]. A plasma channel can be employed as an efficient medium for X-ray lasing [3], harmonic generation [4] or Raman amplification [5]. Furthermore, a recent experiment demonstrated GeV electron acceleration in a channel-guided laser wakefield accelerator for the first time [6]. The principle behind plasma channel guiding is that a plasma column that has a radial density profile with an on-axis minimum can, through the dependence of refractive index on plasma density, act as a lens for laser light [7]. Guiding over long distances is possible due to a balance between the inward bending of light rays through the refractive index gradient and the outward expansion through geometric diffraction. The laser can propagate without significant spot size or centroid oscillations if it couples into a single eigenmode of the channel, in which case it is said to be matched. However, for different spot sizes, off-axis injection or injection under an angle with the channel axis, sizeable spot size or centroid oscillations do occur, and the pulse is called mismatched. Mismatched injection may lead to loss of pulse intensity. Plasma channel guiding is not the only way to achieve a long laser-plasma interaction length: alternative methods include capillary guiding (relying on total internal reflection on the capillary boundary) [8], relativistic self-focusing [9], and laser pulse shaping [10].

As with other types of wave guides, such as optical fibers, it is possible with a plasma channel to guide the light along a curved path by bending the waveguide. This has been experimentally demonstrated by Ehrlich *et al.* for laser pulses with relatively low peak intensities (up to 10^{16} Wcm^{-2}) [11]. The authors provide an analytical estimate for the minimum radius of curvature for confinement the laser pulse to the curved channel. In this paper we discuss the weakly nonlinear regime (laser peak intensities around 10^{17} Wcm^{-2}, for which relativistic and ponderomotive effects start to play a role. We expect that it is not possible to bend laser pulses in the strongly nonlinear regime (peak intensity 10^{18} Wcm^{-2} and above) in curved plasma channels, as it becomes increasingly difficult to radially confine the laser pulse. Furthermore, strong coupling with the wakefield will lead to large losses and pulse deformation. The motivation for this work is to investigate the use of curved plasma channels for electron acceleration, as for example the ability to bend the laser light and/or the electron bunch may be interesting for the design of a multi-stage laser wakefield accelerator. In this paper we only address the propagation of the laser pulse, leaving the electron acceleration dynamics for possible future investigation.

Envelope equation

Here we present the envelope equation that describes the evolution of a laser pulse that propagates in a circular plasma channel. We simplify the geometry of the problem by setting $\partial/\partial y = 0$ in all equations. A radial coordinate r is defined as $r = (x^2+z^2)^{1/2} - R$ with R the radius of the plasma channel and the plasma density is assumed to be parabolic close to $r = 0$: $n_p(r) = n_0 (1+r^2/r_c^2)$, where $r_c \ll R$ determines the curvature of the parabolic density profile. A laser pulse with linear polarization in the y-direction is assumed, and the evolution of the vector potential is described with the wave equation $(c^2\partial^2/\partial x^2 + c^2\partial^2/\partial z^2 - \partial^2/\partial t^2)\, Ay = \omega_p^2\, Ay$ where $\omega_p^2 = 4\pi\, n_p\, e^2/m$ defines the r-dependent plasma frequency ω_p. We introduce the obvious change of coordinates (x,z) to $(r,\phi=\arctan[x/z])$, and assume that Ay is the product of a slowly varying envelope and a rapidly varying carrier wave $eAy/mc^2 = [a(r,\phi,t) \exp(ik_0R\phi - i\omega_0 t) + c.c.]/2$, where a is given in dimensionless form. Furthermore, we introduce a comoving coordinate $s = R\phi - ct$, and find that

$$c^2\left[\frac{\partial^2}{\partial r^2} + \frac{1}{R+r}\frac{\partial}{\partial r} + \frac{R^2}{(r+R)^2}\left(\frac{\partial^2}{\partial s^2} + 2ik_0\frac{\partial}{\partial s} - k_0^2\right)\right]a$$
$$-\left[\frac{\partial^2}{\partial t^2} - 2c\frac{\partial^2}{\partial s\partial t} + c^2\frac{\partial^2}{\partial s^2} - 2i\omega_0\frac{\partial}{\partial t} - \omega_0^2\right]a = \Omega_p^2 a \qquad (1)$$

In the limit $R\rightarrow\infty$, the usual envelope equation is recovered [12]:

$$\left[2i\omega_0\frac{\partial}{\partial t} + 2c\frac{\partial^2}{\partial s\partial t} + c^2\frac{\partial^2}{\partial r^2}\right]a = \Omega_p^2 a \qquad (2)$$

where $\omega_0 = ck_0$ (approximation of very underdense plasma) has been used, and a second-order t-derivative has been omitted (slowly varying envelope approximation).

Paraxial approximation

As a first step, effects related to finite laser pulse length have been omitted, i.e. $\partial/\partial s = 0$ is assumed (paraxial approximation). Keeping terms to lowest order in r/R gives

$$\left[2i\omega_0\frac{\partial}{\partial t} + c^2\frac{\partial^2}{\partial r^2}\right]a = \left[\omega_p^2 - 2\omega_0^2\frac{r}{R}\right]a \qquad (3)$$

From the similarity between Eq. (3) and the 1-particle Schrödinger equation, one can see that the quantity between brackets on the right hand side of the equation plays the role of a potential. Therefore it makes sense to introduce an effective density $n = n_p - 2n_{cr}\, r/R$, which is proportional to this potential, where n_{cr} is the critical density. The minimum of the effective density, which defines the equilibrium position of the laser pulse, is located at $r = (\omega_0/\omega_{p0})^2\, r_c^2/R$, where $\omega_{p0} = \omega_p$ $(r = 0)$.

This implies that a laser pulse injected around $r = 0$, which is the usual condition for matching in a straight channel, will be mismatched and undergo a radial oscillation around the equilibrium position. If the amplitude of this oscillation is large, the approximation of a parabolic channel may break down.

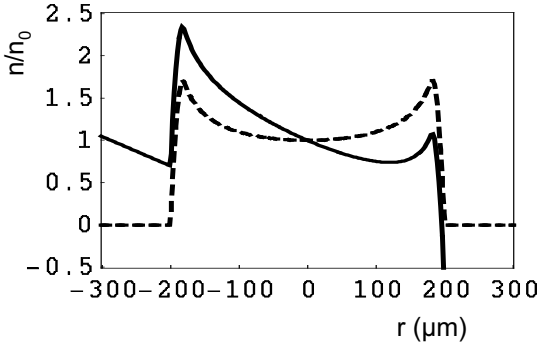

Figure 1. Radial density profile of a curved plasma channel (dashed line) and corresponding effective density for $R = 1$ m (solid line).

In a realistic plasma channel, this would lead to attenuation of the laser pulse due to leakage from the channel. The shift in equilibrium position should be small compared with the channel radius, which requires $r_c/R \ll (\omega_{p0}/\omega_0)^2$. This is a much stronger requirement than the condition $r_c/R \ll 1$ stated above. We illustrate this point by introducing a realistic density profile in Fig. 1, which is modelled after the profile of a slow capillary discharge plasma channel[13,14] with a 200 μm radius and a bottom density $n_0 = 10^{18}$ cm^{-3}. Also shown is the effective density profile for a curved channel with $R = 1$ m. In our simulations, the initial conditions for the laser pulse are

$$a(r) = a_0 \exp[-(r - r_0)^2 / 2r_1^2] \qquad (4)$$

First, we consider the initial conditions for a laser pulse that is matched to a non-curved channel $r_0 = 0$, $r_1 = (cr_c/\omega_{p0})^{1/2} = 43$ μm, $a_0^2 = 0.5$. Because of a relatively large shift in equilibrium position, consistent with $r_c/R = 0.6\ (\omega_{p0}/\omega_0)^2$, we expect to observe strong centroid and spot size oscillations, as well as loss of laser pulse intensity due to leakage of radiation, as shown in Fig. 2a. In order to avoid centroid oscillations altogether, we propose to inject the laser pulse off-axis, around the equilibrium position. Fig. 2b shows the simulation result for $r_0 = 120$ μm (which is the local minimum of the effective density), $r_1 = 43$ μm, $a_0^2 = 0.5$. We still observe centroid and spot size oscillations, but they are not as severe as those found in Fig. 2a. Also, there is no appreciable attenuation. We do, however, observe a periodic deformation of the pulse shape from Gaussian into different asymmetric shapes. This is most likely caused by the asymmetric form of the effective density, for which the parabolic approximation is valid in a much smaller region around the equilibrium position than in the case of a straight channel (see Fig. 1). Also, the curvature at the equilibrium position is larger for the curved channel than for the straight channel. Thus it should be possible to reduce centroid and spot size oscillations even further by using a smaller spot size and perhaps adjusting the injection position. This is confirmed by the simulation result shown in Fig. 2c, which corresponds to $r_0 = 115$ μm, $r_1 = 30$ μm, $a_0^2 = 0.5$. Note also that there is much less pulse shape deformation than in Fig 2b.

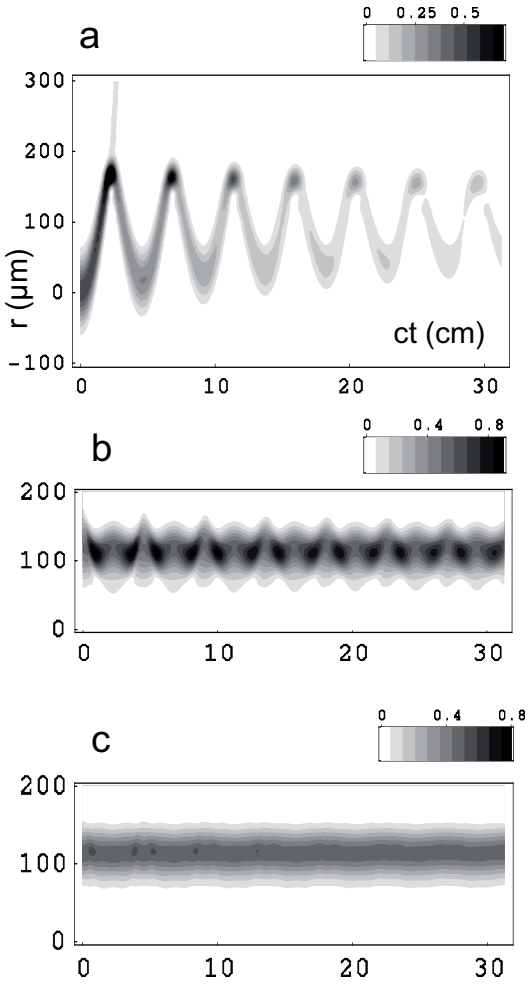

Figure 2. Contour plots of the evolution of $|a|^2$ in a curved plasma channel for 3 different initial conditions: a) $r_0 = 0$, $r_1 = (cr_c/\omega_{p0})^{1/2} = 43$ μm, b) $r_0 = 120$ μm, $r_1 = 43$ μm, c) $r_0 = 115$ μm, $r_1 = 30$ μm. In all cases $a_0^2 = 0.5$.

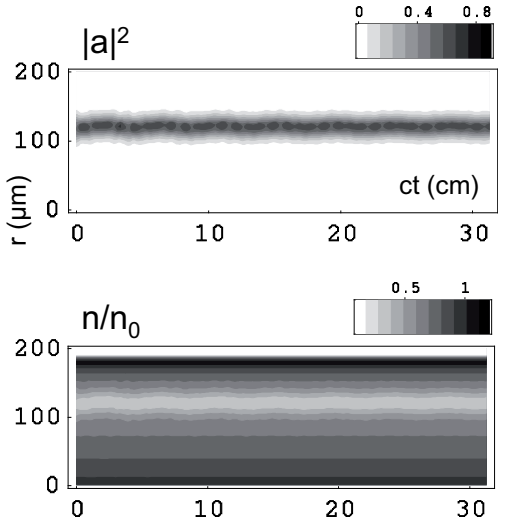

Figure 3. Contour plots of the evolution of $|a|^2$ (top) and effective density (bottom) with self-focusing. Initial conditions: $r_0 = 120$ μm, $r_1 = 20$ μm, $a_0^2 = 0.5$.

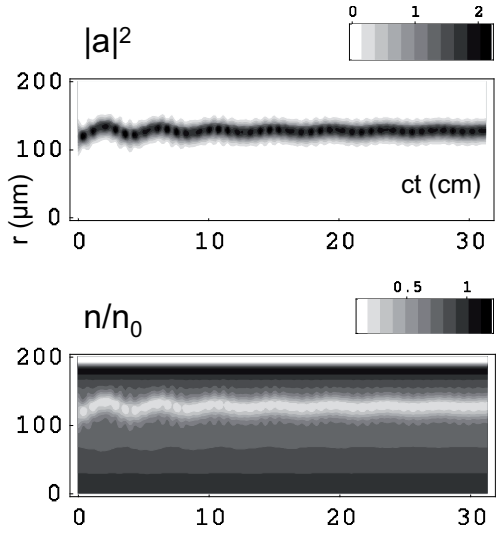

Figure 4. Contour plots of the evolution of $|a|^2$ (top) and effective density (bottom) with self-focusing. Initial conditions: r_0 = 120 μm, r_1 = 20 μm, a_0^2 = 1.2.

For a laser pulse in the relativistic regime (i.e. a_0 of order 1) one has to consider the effect of self-focusing. For simplicity, we consider only relativistic self-focusing, i.e. the change of refractive index due to the relativistic mass correction that stems from the quiver motion, and leave out ponderomotive self-focusing, i.e. radial electron blowout due to the light pressure. For a thorough discussion of both types of self-focusing, see Refs.[15] and[16]. Relativistic self-focusing is modelled by changing the $\omega_p^2 a$-term in Eq. (3) to $\omega_p^2 a/(1+|a|^2)^{1/2}$. As a consequence, the effective density becomes $n = n_p/(1+|a|^2)^{1/2} - 2n_{cr}\, r/R$. As we expect the matched spot size for the self-focusing case to be smaller than without self-focusing[15,16], we select the initial conditions r_0 = 120 μm, r_1 = 20 μm for two different pulse intensities, corresponding to a_0^2 = 0.5 and a_0^2 = 1.2, and we present the simulation results in Figs. 3 and 4, respectively. These Figures show the evolution of $|a|^2$ and the effective density. Due to the feedback from the laser pulse on the effective density, the centroid and spot size oscillations are seen to be damped, and the system evolves towards an equilibrium. At high intensity (the case a_0^2 = 1.2) we observe that the equilibrium position is further from the axis and the equilibrium spot size is smaller than at low intensity (a_0^2 = 0.5). These results can be understood as follows. If the peak of the laser pulse is at the equilibrium position, i.e. at the minimum of the effective density, then that position is found to be $r_0 = (1+a_0^2)^{1/2}(\omega_0/\omega_{p0})^2 r_c^2/R$ where we have used a parabolic approximation for the channel density profile and Eq. (4) for the laser pulse. Thus the equilibrium position r_0 is seen to be further from the axis than in the case without self-focusing, and more and more so with increasing pulse intensity. This confirms that very intense pulses cannot be confined in curved plasma channels due to self-focusing effects, as stated in the Introduction. Close to $r = r_0$ we may write the effective density as $n/n_0 = C + (r-r_0)^2/t_c^2$, where C is a constant and t_c determines the curvature. The matching condition for the laser spot size is $r_1 = (ct_c/\omega_{p0})^{1/2}$, which can be used to determine t_c self-consistently. It is found that t_c/r_c is smaller than 1 and decreases with increasing a_0.This implies that the spot size is smaller than without self-focusing, and decreases with increasing intensity.

Finite pulse length

We retain the longitudinal dependence in Eq. (1) and model the energy loss to the plasma by taking into account the effect of the wakefield. Again, we assume to be in a weakly nonlinear regime, so that a linear hydrodynamic description of the wakefield is adequate. It turns out that, to leading order, the wakefield equations in a curved channel are identical to the ones in a straight channel, which were derived in Ref.[17]:

$$\left[\frac{\partial^2}{\partial s^2} - \frac{\partial^2}{\partial r^2} - \frac{\partial^2}{\partial r \partial s}\left(\frac{c^2}{\omega_p^2}\frac{\partial^2}{\partial r \partial s}\right) + \frac{\omega_p^2}{c^2}\right]\psi = \left(\frac{\omega_p^2}{c^2} - \frac{\partial^2}{\partial r^2}\right)\frac{|a|^2}{4} \quad (5)$$

where Ψ denotes the wakefield potential. To lowest order in r/R, the envelope equation becomes

$$\left[2i\omega_0\frac{\partial}{\partial t} + 2c\frac{\partial^2}{\partial s \partial t} + c^2\frac{\partial^2}{\partial r^2}\right]a = \left[\Omega_p^2 - 2\frac{r}{R}\left(\omega_0^2 - 2c\omega_0\frac{\partial}{\partial s} - c^2\frac{\partial^2}{\partial s^2}\right)\right]a \quad (6)$$

where $\Omega_p(r,s,t)$ is a localized plasma frequency that takes into account the coupling between the laser pulse and the plasma wave. In terms of the wakefield potential, it is expressed as $\Omega_p^2 = \omega_p^2(1 - \Psi) + c^2\partial^2\Psi/\partial r^2$. We have numerically simulated laser pulse propagation by solving the coupled equations (5) and (6). A double Gaussian laser profile

$$a(r,s) = a_0 \exp[-(r - r_0)^2/(2r_1^2) - s^2/(2s_1^2)] \quad (7)$$

is taken as initial condition, with s_1 = 9 μm, a_0^2 = 0.05, r_0 = 115 μm, r_1 = 30 μm (matched pulse) and r_0 = 55 μm, r_1 = 35 μm (mismatched pulse). The simulation results are presented in Figures 5 and 6 in the form of contour plots of $|a|^2$ integrated over r and s, which reveal the longitudinal and transverse envelope dynamics. In these Figures, it is convenient to use a longitudinal coordinate $\sigma = R\phi - vt$ with some $v<c$ to cancel the slippage that occurs in the $s = R\phi - ct$ -frame. This slippage is partly due to the laser pulse group velocity being less than c, and partly a geometric effect, as points of constant s move with velocity $(1+r/R)c$ in the ϕ-direction. For our simulations, it turns out that $v/c = (1-1/\gamma^2)^{-1/2}$ with $\gamma \approx 33$ is a good choice to track the laser pulse (for comparison, $\omega_0/\omega_{p0} \approx 41$).

As expected, the $\int |a|^2\, d\sigma$-plots of the transverse envelope dynamics show large centroid oscillations in the case of a mismatched pulse (Fig. 6), and relatively small centroid and spot size oscillations for a matched pulse (Fig. 5). For the explanation of the observed drift of the centroid towards the axis, we refer to our paper in Phys. Plasmas[18]. The $\int |a|^2\, dr$-plots of the longitudinal envelope dynamics show the formation of a narrow peak towards the end of the pulse at about ct = 13 cm and a subsequent broadening of this feature. This behaviour is typical for the evolution of the laser pulse in a resonant laser wakefield accelerator, which has an initial pulse length of about half of the plasma wavelength to maximize the wakefield amplitude. In our case the initial pulse length is only

slightly longer, and the pulse evolution is very similar[19]. The peak formation is a characteristic of an explosive instability caused by the mutual interaction between the laser pulse and its own wakefield[20]. The most striking difference between the longitudinal dynamics plots of Fig. 5 and Fig. 6 is the pulse oscillation observed in Fig. 6. This is most likely caused by the geometric effect described above: points of constant s (or σ) have a velocity in the ϕ-direction that depends on r, so if the pulse experiences appreciable centroid oscillations, as observed in the transverse dynamics plot of Fig. 6, this will also result in oscillations in the σ-frame. Note also that both oscillations in Fig. 6 have the same period.

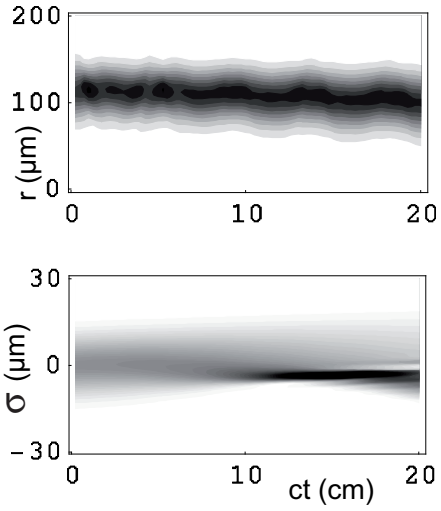

Figure 5. Contour plots of the evolution of $\int |a|^2 d\sigma$ (top) and $\int |a|^2 dr$ (bottom). Initial conditions: r_0 = 115 μm, r_1 = 30 μm, s_1 = 9 μm, and a_0^2 = 0.05.

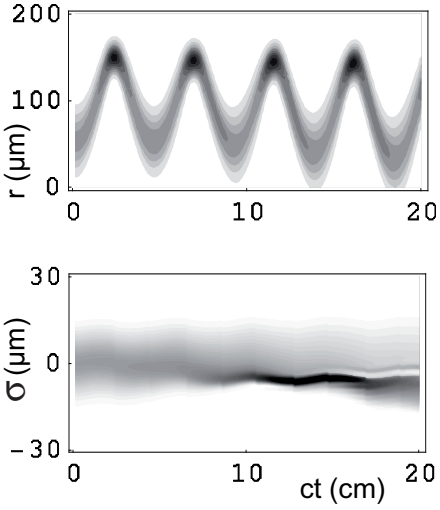

Figure 6. **Contour plots of the evolution of $\int |a|^2 d\sigma$ (top) and $\int |a|^2 dr$ (bottom). Initial conditions: r_0 = 55 μm, r_1 = 35 μm.**

Summary

In this paper, analytical and numerical studies of bending of laser light in a curved plasma channel have been presented. The laser pulse envelope dynamics in a plasma channel has been studied in the paraxial approximation. Pulse propagation in a channel with a relatively small radius of curvature and a realistic plasma density profile has been simulated to demonstrate how large-amplitude centroid oscillations can lead to attenuation. Off-axis injection of the laser pulse around its equilibrium position has been proposed as a means of avoiding these centroid oscillations, as illustrated in Fig. 2. Furthermore, relativistic self-focusing and its effect on the equilibrium position and spot size have been discussed. The equilibrium position has been found to shift outward and the equilibrium spot size to decrease with increasing pulse intensity. Subsequently, finite pulse length effects and wakefields have been included. A near-resonant pulse length has been chosen and it has been found that the longitudinal envelope dynamics are very similar to those of a pulse in a straight channel. The simulation results for the transverse envelope dynamics have been found to be similar to the results in the paraxial approximation.

References

1. P. Sprangle, E. Esarey, J. Krall and G. Joyce, *Phys. Rev. Lett.* **69**, 2200 (1992).
2. D. Spence and S. Hooker, *Phys. Rev. E* **63**, 015401 (2000).
3. J. J. Rocca, V. Shlyaptsev, F. G. Tomasel, O. D. Cortázar, D. Hartshorn and J. L. A. Chilla, *Phys. Rev. Lett.* **73**, 2192 (1994).
4. A. Rundquist, C. G. Durfee III, Z. Chang, C. Herne, S. Backus, M. M. Murnane and H. C. Kapteyn, *Science* **280**, 1412 (1998).
5. Y. Ping, I. Geltner, A. Morozov, N. J. Fisch and S. Suckewer, *Phys. Rev. E* **66**, 046401 (2002).
6. W. P. Leemans *et al.*, *Nature Physics* **2**, 696 (2006).
7. C. G. Durfee III and H. Milchberg, *Phys. Rev. Lett.* **71**, 2409 (1993).
8. C. Courtois, A. Couairon, B. Cros, J. R. Marquès and G. Matthieussent, *Phys. Plasmas* **8**, 3445 (2001).
9. G-Z. Sun, E. Ott, Y. C. Lee and P. Guzdar, *Phys. Fluids* **30**, 526 (1987).
10. E. Esarey, P. Sprangle, J. Krall, A. Ting and G. Joyce, *Phys. Fluids B* **5**, 2690 (1993).
11. Y. Ehrlich, C. Cohen, A. Zigler, J. Krall, P. Sprangle and E. Esarey, *Phys. Rev. Lett.* **77**, 4186 (1996).
12. J. H. Cooley, T. M. Antonsen Jr., C. Huang, V. Decyk, S. Wang, E. Dodd, C. Ren, W. B. Mori and T. Katsouleas, *AIP Conference Proceedings* **647**, 232 (2002).
13. N. A. Bobrova, A. A. Esaulov, J-I. Sakai, P. V. Sasorov, D. J. Spence, A. Butler, S. M. Hooker and S. V. Bulanov, *Phys. Rev. E* **65**, 016407 (2002).
14. B. H. P. Broks, K. Garloff and J. J. A. M. van der Mullen, *Phys. Rev. E* **71**, 016401 (2005).
15. T. Kurki-Suonio, P. J. Morrison and T. Tajima, *Phys. Rev. A* **40**, 3230 (1989).
16. B. Hafizi, A. Ting, P. Sprangle and R. F. Hubbard, *Phys. Rev. E* **62**, 4120 (2000).
17. N. E. Andreev, L. M. Gorbunov, V. I. Kirsanov, K. Nakajima and A. Ogata, *Phys. Plasmas* **4**, 1145 (1997).
18. A. J. W. Reitsma and D. A. Jaroszynski, *Phys. Plasmas* **14**, 053104 (2007).
19. D. F. Gordon, B. Hafizi, R. F. Hubbard, J. R. Peñano, P. Sprangle and A. Ting, *Phys. Rev. Lett.* **90**, 215001 (2003).
20. S. V. Bulanov, I. N. Inovenkov, V. I. Kirsanov, N. M. Naumova and A. S. Sakharov, *Phys. Fluids B* **4**, 1935 (1992).